during program testing, Drs Busing and Levy for supplying the excellent ORGLS, and to the National Institutes of Health for financial support.

References

ATOJI, M. & LIPSCOMB, W. N. (1959). *J. Chem. Phys.* **31**, 601.
BOER, F. P., STREIB, W. E. & LIPSCOMB, W. N. (1964). *Inorg. Chem.* **3**, 1666.
BUSING, W. R. & LEVY, H. A. (1962). ORGLS. Oak Ridge National Laboratory, TM-271, Oak Ridge, Tennessee.
CRUICKSHANK, D. W. J. (1956*a*). *Acta Cryst.* **9**, 754.
CRUICKSHANK, D. W. J. (1956*b*). *Acta Cryst.* **9**, 757.
DICKERSON, R. E., WHEATLEY, P. J., HOWELL, P. A. & LIBSCOMB, W. N. (1957). *J. Chem. Phys.* **27**, 200.
ENRIONE, R. E., BOER, F. P. & LIPSCOMB, W. N. (1964). *Inorg. Chem.* **3**, 1659.
HIRSHFELD, F. L., ERIKS, K., DICKERSON, R. E., LIPPERT, E. L. & LIPSCOMB, W. N. (1958). *J. Chem. Phys.* **28**, 56.
International Tables for X-ray Crystallography (1962). Vol. III. Birmingham: Kynoch Press.
JACOBSON, R. A., & LIPSCOMB, W. N. (1959). *J. Chem. Phys.* **31**, 605.
LAVINE, L. R., & LIPSCOMB, W. N. (1954). *J. Chem. Phys.* **22**, 614.
MOORE, E. B., DICKERSON, R. E., & LIPSCOMB, W. N. (1957). *J. Chem. Phys.* **27**, 209.
NORDMAN, C. E., & LIPSCOMB, W. N. (1953). *J. Chem. Phys.* **21**, 1856.
PAWLEY, G. S. (1963). *Acta Cryst.* **16**, 1204.
PAWLEY, G. S. (1964). *Acta Cryst.* **17**, 457.
POTENZA, J. A. & LIPSCOMB, W. N. (1964). *Inorg. Chem.* **3**, 1673.
SIMPSON, P. G. & LIPSCOMB, W. N. (1963). *J. Chem. Phys.* **39**, 26.
VOET, D. & LIPSCOMB, W. N. (1964). *Inorg. Chem.* **3**, 1679.

Acta Cryst. (1966). **20**, 638

Trioctahedral One-Layer Micas. III. Crystal Structure of a Synthetic Lithium Fluormica*

BY HIROSHI TAKEDA† AND J. D. H. DONNAY

The Johns Hopkins University, Baltimore, Maryland 21218, *U.S.A.*

(*Received* 14 *July* 1965)

The crystal structure of a synthetic lithium fluormica, between $K(Mg_2Li)Si_4O_{10}F_2$ and $KMg_3(Si_3Al)O_{10}F_2$ in composition but potassium deficient, was determined and refined from three-dimensional photometer data and $0kl$ counter data. The site occupancies of octahedral and interlayer positions were also refined to establish the final chemical formula. In keeping with the small c/b of fluormicas, the structure shows flattening of the octahedral sheet, little ditrigonality in the basal oxygen rings of the tetrahedral sheets, and flattening of the oxygen octahedron around potassium. As to interatomic distances, F–F (2·629 Å) is shorter than O–O (2·804 Å), so that fluorine and oxygen ions are not coplanar. Inner and outer K–O distances average 2·995 and 3·278 Å respectively.

Introduction

It remains as important as ever to accumulate data on the crystal structures of micas, if we are to understand the polymorphism of this mineral group. Few mica structures have been refined. No refined structure is available either for a lithium mica or for a fluormica. The lepidolites, which contain both lithium and fluorine, are of special interest because of their many polymorphs. The synthetic polylithionite, which we had hoped to study, never yielded any single crystal suitable for X-ray work. We had also hoped to refine the structure of synthetic taeniolite, which would have had the advantage of having only silicon in the tetrahedra, as opposed to ferri-annite and ferriphlogopite, in which ferric iron substitutes for silicon (Donnay, Donnay, & Takeda, 1964), but our sample turned out not to be pure taeniolite: aluminum substitutes for silicon, less lithium is present, and potassium is deficient. The site occupancies were refined by least squares, along with the structural parameters.

Experimental

The sample, which Dr H. S. Yoder, Jr. kindly gave us for investigation, was synthesized by the Mycalex Corporation of America. The process used is briefly described in a letter from E. V. deVilleroy (private communication, 1963):

'A charge of blended raw materials is fed in an electric furnace. Large graphite electrodes produce the needed heat. Heat is applied at the center of the charge under

* Work supported by the National Science Foundation (NSF.GP.1565).

† On leave of absence from the Mineralogical Institute, University of Tokyo, Hongo, Tokyo, Japan.

precise control, so that the mass is completely fused but an outside crust remains. After cooling, the outer shell is removed leaving pure mica crystals'.

The crystals are transparent, colorless, platy parallel to (001), up to 1 cm across and 3 mm in thickness. The (001) micaceous cleavage is eminent, very easy, and elastic. The cell dimensions, obtained by the precession method, are very close to those of fluorphlogopite (Table 1). The cell volume is 487·9 Å^3. The diffraction aspect is $C*/*$; space group $C2/m$ was assumed and, on refinement, turned out to be correct.

About 200 mg of clear crystals, with the same physical appearance as that of the crystal used for collecting diffraction intensities, were hand-picked under the binocular microscope. The chemical analysis (U.S. Bureau of Mines, Norris, Tennessee) gave the following weight percentages:

SiO_2	Al_2O_3	Fe_2O_3	MgO	
56·13	3·15	0·12	22·19	
K_2O	Li_2O	F	O=F	Total
9·86	1·97	9·40	−3·96	98·86,

corresponding to the following formula, for this bulk composition:

$$(K_{0.86}\square_{0.14})(Mg_{2.26}Al_{0.08}Li_{0.54})(Si_{3.83}Al_{0.17})O_{10}F_{2.03}. \quad (1)$$

It shows that our sample differs from taeniolite (Table 1) in three respects: (1) deficiency of potassium; (2) excess of magnesium; (3) presence of aluminum. A qualitative electron-probe analysis, performed on clear crystals from the original batch, confirmed the presence of a notable amount of aluminum (P. Iber, private communication, 1964). Another check on the reliability of chemical formula (3) is afforded by a comparison of densities. A large, clear crystal, selected from the batch, gave D_m 2·82 g.cm^{-3}. The calculated value, for chemical formula (3), is D_x 2·832; for the bulk composition (1), D_x 2·761 g.cm^{-3}. For a synthetic fluorphlogopite, Kohn & Hatch (1955) give a measured value of 2·882 g.cm^{-3}.

The intensity data were collected by three different methods: (1) Integrated Weissenberg photographs, with triple film and copper foil between films, were taken in Mo $K\alpha$ radiation (0·7107 Å) about the a axis (h= 0 to 6), with the integrating cassette designed by Nordman & Patterson (1957). (2) In order to provide measurements of very weak intensities, overexposed non-integrated Weissenberg films were prepared about the a axis (Cu $K\alpha$ for h=0 to 3; Mo $K\alpha$ for h=4 to 6) and about the b axis (Mo $K\alpha$ for k=0 to 2), as well as overexposed precession photographs in Mo $K\alpha$ radiation (b axis, k=0 to 3; c axis, l=0 to 2; a axis, h=0). The integrated photographic intensities were measured on a micro-photodensitometer; the non-integrated ones were estimated visually with the help of an intensity calibration strip. (3) For comparison the 63 reflections $0kl$ were measured (Cu $K\alpha$) with a scintillation counter and a pulse-height analyzer on the Supper non-automated single-crystal diffractometer, based on the Weissenberg geometry. The same crystal was used throughout; it measures 0·34 by 0·20 by 0·07 mm.

The photographic intensities were processed on the IBM 7094 computer, by our data-reduction program, which calculates net integrated intensities, applies absorption, Lorentz and polarization corrections, and converts the intensities to observed amplitudes. The absorption correction is made by computing the transmission factor by means of the GNABS subroutine (Burnham, 1963*b*): with a linear absorption coefficient of 12·16 for Mo $K\alpha$ radiation, the transmission factors are found to lie between 0·93 and 0·82.

The standard deviation of the observed amplitude F_o for every set hkl of n symmetrically related observed reflections is calculated as follows. For each measured intensity the mean range of deviations is first estimated from the fluctuations of the pen of the photometer recorder. This value is then converted to the F_o scale by the data-reduction program, and the standard deviation of the measurement is estimated as one half of the mean range on the F_o scale. The root-mean-square value s is then calculated for the n measurements in the set hkl. This value s is compared with the standard deviation σ of the mean value $\bar{F}_o$ of the n measurements (which is the r.m.s. value of the deviations of the measured F_o's from $\bar{F}_o$). If $\sigma < s$, we take s as standard deviation of the F_o; if $s < \sigma$, we take $\sqrt{(s^2+\sigma^2)/2}$. Reflections that could not be observed on *any* photograph were assigned an intensity $\frac{1}{2}I_{\min}$, where $I_{\min}$ is the minimum observable, and a standard deviation $\sigma = 0{\cdot}298\ I_{\min}$.

Table 1. *Cell dimensions and chemical formulae of synthetic fluormicas*

Taeniolite $K(Mg_2Li)Si_4O_{10}F_2$	5·27	9·13	10·25	100°	Yamzin *et al.* (1955)
Magnesian taeniolite $(K_{0.65}\square_{0.35})(Mg_{2.40}Li_{0.63})Si_{3.98}O_{10.01}F_{1.99}$	5·227	9·057	10·133	99° 52′	Miller & Johnson (1962)
*Lithian fluorphlogopite $(K_{0.95}\square_{0.05})(Mg_{2.80}Li_{0.20})(Si_{3.25}Al_{0.75})O_{10}F_2$	5·31	9·21	10·13	100° 01′	Present paper
Fluorphlogopite $KMg_3(Si_3Al)O_{10}F_2$	5·310	9·195	10·136	100° 04′	Yoder & Eugster (1954)

* The chemical formula given is formula (3), established by X-ray diffraction. The chemical analysis gave a bulk composition formula (1). The standard deviations on cell parameters are : $\sigma(a)=0{\cdot}016$, $\sigma(b)=0{\cdot}028$, $\sigma(c)=0{\cdot}030$ Å, $\sigma(\cos\beta)=0{\cdot}0022$.

The diffractometer intensities were converted to observed amplitudes, duly corrected by Lorentz and polarization factors, and the standard deviations were computed, by means of Burnham's (1963*b*) data-reduction program. The absorption correction is made by Burnham's GNABS subroutine with a linear absorption coefficient of 117·57 for Cu $K\alpha$ radiation.

Structure determination and refinement

The trial structure was first computed by our structure-prediction program (Donnay, Donnay & Takeda, 1964*b*), written for the IBM 7094 computer. The prediction of this trioctahedral 1*M*-mica structure, in $C2/m$, is based on the cell dimensions and composition (Table 1) of synthetic taeniolite (Yamzin, Timofeyeva, Shashkina, Belova & Gliki, 1955), the necessary bond lengths being taken from *International Tables for X-Ray Crystallography* (1962, 258–260). Our model assumes $Z=2$ and the equivalence of all octahedra. Four magnesium and two lithium ions were thus distributed at random over the six sites of position 2(*c*) and position 4(*h*).

The atomic scattering factors were taken from *International Tables* (1962, p.202), silicon and oxygen atoms being considered half-ionized and all the others completely ionized. The full-matrix least-squares refinement program ORFLS (Busing, Martin, & Levy 1962) was used throughout.

Two-dimensional refinements

At first we used only the 0*kl* diffractometer intensities and the trial structure gave $R=0{\cdot}302$ for all 63 reflections in the zone, with isotropic temperature factors of 0·5 for $(Mg_{2/3}Li_{1/3})$, 0·5 for Si, and 1·0 for all other atoms. The refinement was started by letting the y and z coordinates vary. Later on the multipliers of the two atomic scattering factors f of the octahedral positions were also allowed to vary. The concept of multipliers (Busing, Martin & Levy, 1962) is particularly suited to the study of solid solutions. In the present case, the scattering factors of the two octahedral positions each had to be multiplied by a number greater than one, which means that the Mg:Li atomic ratio must increase over the initial 2:1 in each position. This result indicates that our crystal must contain more magnesium than appears in the taeniolite formula. The bulk composition given by chemical analysis (1) indeed shows the Mg:Li atomic ratio to be 2·26:0·54. For the charges to balance, this substitution of magnesium for lithium requires the replacement of silicon by an element of lower valence, such as aluminum, or a deficiency in potassium, or both. Note that charge balance cannot be achieved by substituting oxygen for fluorine, because the analysis does not support this replacement; in fact the little amount of substitution that is reported occurs in the opposite direction – fluorine for oxygen. The original taeniolite formula must be rewritten as follows:

$$(K_{1-(p-q)}\square_{p-q})(Mg_{(2+p')/3}Li_{(1-p')/3})^{(1)}$$
$$(Mg_{(2+p'')/3}Li_{(1-p'')/3})_2^{(2)}(Si_{(4-q)/4}Al_{q/4})_4O_{10}F_2, \quad (2)$$

where

$$p=(p'+2p'')/3$$

and the superscripts (1) and (2) indicate positions 2(*c*) and 4(*h*) respectively.

Another way of showing that the taeniolite formula does not apply to this crystal is to keep every multiplier equal to unity (that is, keep the composition constant) and let the coordinates and the individual atomic temperature factors vary. This was done, and the refinement could not proceed because the temperature factors B of the octahedral positions 2(*c*) and 4(*h*) became negative whereas all the other B's were normal (Burnham, 1965).

With formula (1) and the corresponding atomic scattering factors, the same refinement (Table 3*a*) still led to unsatisfactory B's, although the residual R improved considerably (Table 2, line 2). For this and other residuals based on the 0*kl* reflections only, 59 extinction-free reflections were taken into consideration out of a total of 63. Reasonable B's were first obtained by changing the composition, that is, determining p', p'', and q by trial-and-error (Table 2, line 3). The best chemical formula was finally established, from two-dimensional data, by successive least-squares refinements of three groups of variables: (1) scale factor; (2) atomic coordinates Y/b and Z/c together with individual B's; (3) multipliers of atomic scattering factors. For each crystallographic position there are two multipliers, the sum of which is equal to unity. They are the fractions of site occupancy pertaining to the two atomic species: K and □, Mg and Li, Si and Al. They are therefore equal to the subscripts of the appropriate elements in each parenthesis in formula (2). As a matter of computational technique, all parameters (multiplier, X/a, Y/b, Z/c, B) were supplied twice for every position with double occupancy (once for each atomic species in the postion); the parameters (other than multiplier) of the heavier atom were refined, and those of the lighter atom were set equal to those of the heavier one after every cycle of refinement. As regards multipliers, those of K, Mg(1), and Mg(2) were refined and that of Si was derived from them. After each refinement cycle, if m was the value of the multiplier for a Mg atom, the multiplier of the corresponding Li atom was set equal to $(1-m)$. This method of computation simply required writing an appropriate patch subroutine, to be inserted as RESETX in the ORFLS program. The result (Table 2, line 4) shows a low residual and temperature factors B that are very satisfactory, judging from other structures. The yz projection of the structure is well resolved, without any overlap of atoms.

As a check, we repeated the refinement on the assumption that the composition was that of fluorphlogopite (Table 1), in the hope that R would increase and the temperature factors of the Mg ions would become worse. This was indeed observed (Table 2, line 5).

The chemical formula thus established by the two-dimensional refinement was finally retained, after comparison with the results of three-dimensional refinements. It is

$$(K_{0\cdot95}\square_{0\cdot05})(Mg_{2\cdot80}Li_{0\cdot20})(Si_{3\cdot25}Al_{0\cdot75})O_{10}F_2\,. \qquad (3)$$

Three-dimensional refinements

The x coordinates and the scale factors were determined layer by layer ($h=0$ to 6), using the approximate chemical composition that had been found by trial-and-error (Table 2, line 3), because the results of the chemical analysis were not available at the time. Then we refined the x, y, z coordinates, the scale factors, and the isotropic individual temperature factors, using formula (1) of the bulk composition and keeping it fixed (Table 3*a*). In this and in the next run, the intensity data adopted for the $0kl$ reflections were the averages of the values obtained by photography and by diffractometry, weighted one to one; photographic data only were available for the other reflections, for which the weight was taken as $1/2\sigma^2$. The R value was obtained

Table 2. *Chemical composition, apparent temperature factors, and residual for several refinements*

No.	Chemical composition p'	p''	p	q	Apparent temperature factors (Mg,Li)(1)	(Mg,Li)(2)	(Si,Al)	(K,□)	Residual R
1	0	0	0	0	0·5	0·5	0·5	1·0	0·302
2	0·340	0·340	0·340	0·168	0·09	−0·07	1·06	1·85	0·075
3	0·700	0·850	0·800	0·667	0·66	0·59	0·73	1·65	0·056
4	0·774	0·820	0·805	0·746	0·68	0·64	0·74	2·12	0·048
5	1·000	1·000	1·000	1·000	1·00	0·96	0·67	2·42	0·057
6	0·340	0·340	0·340	0·168	0·01	−0·07	0·76	1·73	0·091
7	0·803	0·851	0·835	0·735	0·51	0·58	0·70	2·38	0·082

Trial structure:
1. Taeniolite formula; temperature factors fixed.

Two-dimensional refinements:
2. Bulk composition.
3. Trial and error.
4. Least squares.
5. Fluorphlogopite formula.

Three-dimensional refinement:
6. Bulk composition.
7. Least squares; 4 cycles.

Table 3(*a*). *Preliminary atomic coordinates and isotropic temperature factors obtained with bulk composition*

Position	K 2(*b*)	O(1) 4(*i*)	O(2) 8(*j*)	(Si,Al) 8(*j*)	O(3) 8(*j*)	F 4(*i*)	(Mg,Li)(1) 2(*c*)	(Mg,Li)(2) 4(*h*)
				Two-dimensional refinement				
Y/b	½	0	0·2306	0·1671	0·1657	½	0	0·3314
Z/c	0	0·1665	0·1661	0·2247	0·3921	0·4032	½	½
B	1·85	1·02	1·13	1·06	1·35	1·39	0·09	−0·007
				Three-dimensional refinement				
X/a	0	0·0236	0·3215	0·0751	0·1306	0·1330	0	0
Y/b	½	0	0·2348	0·1665	0·1662	½	0	0·3312
Z/c	0	0·1657	0·1671	0·2250	0·3918	0·4027	½	½
B	1·73	1·43	1·38	0·76	0·84	1·02	0·01	−0·07

Table 3(*b*). *Atomic coordinates and temperature factors of lithian fluorphlogopite*

B, isotropic temperature factor (in Å²); β_{ij}, anisotropic parameters in the expression

$$\exp-\{\beta_{11}h^2+\beta_{22}k^2+\beta_{33}l^2+\beta_{23}2kl+\beta_{31}2lh+\beta_{12}2hk\}.$$

In Tables 3(*b*) to 8, the standard deviations given between parentheses are expressed in units of the last digit stated.

Position	K 2(*b*)	O(1) 4(*i*)	O(2) 8(*j*)	(Si,Al) 8(*j*)	O(3) 8(*j*)	F 4(*i*)	(Mg,Li)(1) 2(*c*)	(Mg,Li)(2) 4(*h*)
X/a	0	0·0235 (7)	0·3218 (4)	0·0753 (2)	0·1305 (4)	0·1329 (5)	0	0
Y/b	½	0	0·2346 (3)	0·1665 (1)	0·1665 (3)	½	0	0·3308 (2)
Z/c	0	0·1664 (4)	0·1670 (2)	0·2250 (1)	0·3910 (2)	0·4020 (3)	½	½
β_{11}	0·0195 (7)	0·178 (13)	0·0134 (8)	0·0066 (3)	0·0053 (7)	0·0100 (9)	0·0043 (7)	0·0047 (5)
β_{22}	0·0073 (3)	0·0043 (5)	0·0050 (3)	0·0018 (1)	0·0028 (3)	0·0023 (3)	0·0010 (3)	0·0011 (2)
β_{33}	0·0048 (2)	0·0021 (4)	0·0024 (2)	0·0019 (1)	0·0026 (2)	0·0032 (3)	0·0017 (2)	0·0018 (2)
β_{23}	0	0	−0·0006 (3)	−0·0002 (1)	−0·0001 (2)	0	0	0
β_{31}	0·0014 (3)	−0·0004 (6)	0·0015 (4)	0·0007 (1)	0·0009 (3)	0·0005 (4)	0·0006 (3)	0·0009 (2)
β_{12}	0	0	−0·0016 (5)	0·0004 (2)	−0·0006 (4)	0	0	0
B	2·13 (4)	1·42 (6)	1·30 (4)	0·70 (1)	0·85 (4)	1·10 (5)	0·53 (4)	0·55 (3)

for all reflections (Table 2, line 6) inside a limiting sphere corresponding to $\sin\theta=0{\cdot}5$ for Mo $K\alpha$ radiation.

The next run was to do the least-squares refinement (four cycles), letting the multipliers of the cationic scattering factors vary, together with the other parameters. The results (Table 2, line 7) show no great departure from the preceding ones (line 4), as regards temperature factors and composition. At this stage a three-dimensional electron-density function was computed in sections parallel to (010), by means of our JHORTFR program (Donnay & Takeda, 1964), which prints undeformed Fourier maps. All peaks have their expected heights and the background is uniformly low. (It may be remarked that these maps can be interpreted at a glance, without being contoured, as the printing itself brings out the

Table 4. *Bond lengths and angles in the tetrahedral sheet*

All angles have a common apex at (Si,Al). O(1) and O(2) are basal, O(3) is apical.

	(Si,Al)	O(1)	O(2)	O(3)
O(1)	1·650 Å (5)	—	—	2·721 Å (7)
				110·75° (17)
O(2)	1·649 (4)	2·679 Å (7)	—	2·716 (7)
		108·57° (20)		110·51° (18)
O(2′v)	1·647 (4)	2·669 (8)	2·670 Å (8)	2·715 (7)
		108·12° (23)	108·22° (22)	110·58° (17)
O(3)	1·656 (6)	—	—	—
Averages	1·651 Å		2·695 Å	
			109·46°	

Table 5. *Bond lengths and angles in the octahedral sheet*

Around (Mg,Li)(1) in position 2(*c*). Site symmetry 2/*m*		Around (Mg,Li)(2) in position 4(*h*). Site symmetry 2	
(Mg,Li)(1)–O(3)	2·078 Å (5)×4	(Mg,Li)(2)–O(3)	2·077 Å (6)×2
(Mg,Li)(1)–F(vii)	2·028 (6)×2	(Mg,Li)(2)–O(3v)	2·063 (5)×2
		(Mg,Li)(2)–F(v)	2·039 (5)×2
Weighted average	2·061 Å	Average	2·060 Å
	Shared edges		
O(3)–O(3′ii)	2·804 Å (8)×2	O(3)—O(3vii)	2·807 Å (7)×2
	84·87° (26)		85·35° (18)
O(3)–F(vii)	2·722 (6)×4	O(3v)–O(3vii)	2·804 (8)×1
	83·06° (16)		85·60° (26)
		O(3)—F(vii)	2·722 (6)×2
Weighted averages	2·749 Å		82·80° (17)
	83·66°	F(v)—F(vii)	2·629 (9)×1
			80·31° (26)
		Weighted averages	2·749 Å
			83·70°
	Unshared edges		
O(3)–O(3″i)	3·067 Å (10)×2	O(3)—O(3v)	3·069 Å (8)×2
			95·65° (18)
O(3)–F′(v)	3·073 (8)×4		
		O(3)—F(v)	3·062 (8)×2
Weighted average	3·071 Å		96·15° (18)
		O(3v)–F(v)	3·074 (10)×2
			97·07° (24)
		Averages	3·068 Å
			96·29°

All angles have a common apex at (Mg,Li).

Table 6. *Bond lengths and angles in the interlayer*

K–O(1iv)	2·990 Å (9)×2	K–O(1′iv)	3·276 Å (9)×2
K–O(2′v)	2·997 (7)×4	K–O(2)	3·279 (7)×4
Weighted average	2·995 Å	Weighted average	3·278 Å
	K–F 4·010 (12)		
O(2)–O(1iv)–O(2i)	132·64° (26)×2	O(2′v)–O(1′iv)–O(2′iv)	107·54° (29)×2
O(2)–O(2′v)–O(1′iv)	132·32° (20)×4	O(1iv)–O(2)–O(2′v)	107·59° (21)×4
Weighted average	132·43°	Weighted average	107·57°

Table 7. *Lateral and basal* O–O *distances in inner oxygen octahedron around* K, *shortest interlayer* O–O *distances, and* O–K–O *angles in synthetic lithian fluorphlogopite*

		Lithian fluorphlogopite (this paper)		Ferri-annite, Donnay *et al.* (1964*a*)	Ferri-phlogopite, Steinfink (1962)
Lateral distances	O(1iv)–O(2^{iv}vii)	4·157 Å	(10)×4	4·23 Å	4·21 Å
	O(2′v)–O(2^{iv}vii)	4·155	(11)×2	4·25	4·21
	Weighted average	4·156		4·237	4·210
Basal distances	O(1iv)–O(2′v)	4·308	(11)×4	4·38	4·11
	O(2′v)–O(2′iv)	4·322	(14)×2	4·44	4·14
	Weighted average	4·313		4·400	4·120
Shortest interlayer distances	O(1iv)–O(1^{iv}vii)	3·337	(13)×4	3·40	3·55
	O(2)–O(2^{iv}vii)	3·349	(11)×2	3·41	3·52
	Weighted average	3·341		3·403	3·540
Angles	O(1iv)–K–O(2^{iv}vii) = 180° − O(1iv)–K–O(2′v)	87·96°	(17)×4	87·98°	91·37°
	O(2′v)–K–O(2^{iv}vii) = 180° − O(2′v)–K–O(2′iv)	87·74	(24)×2	87·50	91·00
	Weighted average	87·89°		87·82°	91·25°

undeformed shape of each peak and one or two ripples around it).

A further refinement of the multipliers, with anisotropic temperature factors, was also carried out at this stage to see whether the composition would change significantly. It did not justify abandoning formula (3).

The last refinement keeps this composition fixed and lets the coordinates and the anisotropic temperature factors vary. The weighting scheme of intensity data was modified as follows: (1) for 0*kl* reflections, the amplitudes obtained by diffractometry and by photography were averaged in the ratio of 4 to 1, and were given, as standard deviation, the square root of the weighted average (4 to 1) of the square of the standard deviations of the two values; (2) other observed reflections were given weight $1/\sigma^2$, instead of $1/2\sigma^2$ as before; (3) for non-observed reflections with calculated structure factors nearly equal to zero, $1/||F_o|-|F_c||$ was used as weight. After adjustment of the scale factors and four cycles of refinement, no further change of parameters took place (Table 3*b*). The final residual is $R=0{\cdot}073$, for all 721 reflections and $R=0{\cdot}046$ for all the 472 observed reflections inside our limiting shpere. Keeping all other parameters as in the final structure, the isotropic individual temperature factors were refined to $R=0{\cdot}078$ (for all reflections) (Table 3*b*); they are comparable to those found previously with a somewhat different composition (Table 2, line 7).

Bond lengths and angles

The parameters and the variance-covariance matrix were used as input data for the Crystallographic Function and Error Program (ORFFE) (Busing, Martin & Levy, 1964) to compute bond lengths and angles (Tables 4 to 7) and the r.m.s. components of the thermal displacements of each basal oxygen atom along the principal axes of its ellipsoid (Table 8). The standard deviations listed in these tables include the errors on the cell dimensions.

Table 8. *Apparent thermal displacements of basal oxygen atoms*

r_i, $i=1, 2, 3$, principal axes of the ellipsoid; λ, μ, υ, direction angles in auxiliary system of coordinates: **a**, **b**, **c***, for atom O(1) and **a**−**b**, 3**a**+**b**, **c***, for atom O(2); r_K = component along **a** for O(1), along **a**−**b** for O(2).

Atom	R.m.s. components		Direction angles λ	μ	υ
O(1)	r_1 0·099 Å	(9)	80° (5)	90° (−)	10° (5)
	r_2 0·136	(7)	90 (−)	180 (−)	90 (−)
	r_3 0·163	(6)	10 (5)	90 (−)	100 (5)
	r_K 0·161	(6)			
O(2)	r_1 0·106	(6)	105 (5)	92 (12)	16 (5)
	r_2 0·126	(5)	87 (7)	177 (10)	92 (12)
	r_3 0·156	(5)	164 (5)	93 (7)	105 (5)
	r_K 0·153	(5)			

Discussion of the structure

The final chemical formula (3) based on X-ray analysis differs slightly according to the method of refinement. The total ranges of variation are as follows: $p=0{\cdot}80-0{\cdot}84$, $q=0{\cdot}75-0{\cdot}67$, with $p-q=0{\cdot}05-0{\cdot}13$.

Let us compare the interatomic distances actually observed in the crystal structure with the distances that would be expected, on the basis of chemical formula (3).

Cation-to-oxygen distances

The average observed tetrahedral-cation-to-oxygen distance is 1·651 Å (Table 4). The calculated value is 1·648 Å, for cationic composition ($Si_{3\cdot25}Al_{0\cdot75}$) and the following literature data: Si–O 1·62, Al–O 1·77 Å

(Smith & Bailey, 1963). Using the same literature data, a composition of $Si_{3\cdot17}Al_{0\cdot87}$ corresponds to the observed distance 1·651 Å. The observed octahedral-cation-to-anion distances (Table 5) give a weighted average of 2·060. The calculated values of $(Mg_{2\cdot80}Li_{0\cdot20})$–O and $(Mg_{2\cdot80}Li_{0\cdot20})$–F weighted in the ratio of 2 to 1 give an average of 2·066, based on the following literature data: Mg–O 2·10, Li–O 2·16, Mg–F 1·99, Li–F 2·011 Å (*International Tables*, 1962, pp.258–260). The refinement shows little enrichment of lithium in the position 2(*c*) but the difference is not significant. As in other micas the K–O distances are of two kinds, due to the ditrigonal configuration of the oxygen rings on either side of the potassium ion. The observed values (Table 6) give weighted averages of 2·995 and 3·278 Å for the inner and the outer K–O distance, respectively. Note that the K–O distances depend on the size of the tetrahedra and on the angle α through which the tetrahedra have been rotated about c^*. In the present mica the relatively small size of the tetrahedra, as compared with the (Si_3Fe) tetrahedra in ferri-annite, and the low value of α (Table 9) account for the small value of the longer of the two K–O distances. The low value of α, the lowest on record for a mica structure, explains why the shorter K–O distance is as large as it is.

Table 9. *Observed and predicted structural elements for synthetic lithian fluorphlogopite*

	Observed	Predicted
(Si, Al)–O	1·651 Å	1·648 Å
(Mg, Li)–(O, F)	2·060	2·066
(O–O) shared	2·749	2·77
(O–O) unshared	3·069	3·07
(O–O)*s*/(O–O)*u*	0·896	0·901
K–O inner	2·995	2·97
K–O outer	3·278	3·38
α	6°13′	8°55′
ψ	59°19′	59°05′

The small c/b ratio

To a first approximation all trioctahedral 1*M* mica structures can be considered the same except for a scale factor, *b* (Donnay, Donnay & Takeda, 1964*b*). The mica structures can be normalized by dividing all the cell dimensions by *b*. A striking feature of the fluorphlogopites is their small *c*/*b* ratio.

The observed facts that can be correlated with the shortening of *c*/*b* are: (1) the flattening of the octahedral layer, that expresses itself in a higher value of the ψ angle (59°19′); (2) the flattening of the inner octahedron of oxygen atoms around potassium, which can be expressed by a similar angle, φ, here equal to 56°16′.

We call inner octahedron the octahedron formed by the six nearest oxygen neighbors of a potassium atom. Franzini & Schiaffino (1963) have mentioned such octahedra in biotite structures, where they are regular or even thickened into trigonal antiprisms. In our lithian fluorphlogopite they are flattened parallel to (001). In such an octahedron we distinguish edges of two kinds: *lateral* and *basal*. They can be compared with the *shared* and *unshared* edges of the (Mg,Li) octahedra, except that the latter form a continuous sheet.

The ratio *s*/*u* of shared to unshared edge is 0·896. The ratio *l*/*b* of lateral to basal edge in the K inner octahedron (Table 7) is 0·964. These ratios afford another way of estimating the flattening of the octahedra; each one is a function of the corresponding angle, ψ or φ (see Donnay, Donnay & Takeda, 1964).

The flattening of the K inner octahedron is also apparent in the low value of the shortest interlayer O–O distance, that is, the distance in which one oxygen atom, on one side of K, belongs to the inner octahedron, whereas the other oxygen atom, on the other side of K, is part of the outer octahedron. (The outer octahedron is formed by the six next-nearest oxygen neighbors of K.) This shortest O–O distance is 3·341 (Table 7).

The flattening of the inner octahedron also affects the value of the O–K–O angle that would be a right angle in a regular octahedron (Table 7).

The interpretation of the above facts leads us to the conclusion that φ is a function of ψ. This can be seen as follows. If, for any reason, the octahedral sheet becomes flattened, that is, has a large ψ, the *b* must be large and α must be small. This means that the oxygen configuration looks more like a hexagon than a ditrigon. As a consequence the K atom can 'fall' into the open hole, to attain the 'proper K–O distance'. In other words, φ is large and the inner octahedron is flattened.

Now what are reasons for a flattening of the octahedral sheet? We see two: (1) The replacement of the octahedral cation Mg by a smaller one; (2) The replacement of OH by F. Either cause will give a smaller d_o cation-to-anion distance, which tends to make the octahedra smaller. In the first case, Mg is replaced, say by Fe^{3+}; the ferric ions, being more highly charged, repel each other and, in so doing, produce a flattening of the octahedral sheet. In the second case, two magnesium ions would tend to approach each other but repel each other and, in so doing, bring about a decrease in the value of the F–Mg–F angle and the flattening of the sheet. In our lithian fluorphlogopite the effect of lithium-for-magnesium substitution is negligible in this respect and the flattening of the octahedral sheet is to be ascribed primarily to the replacement of hydroxyl by fluorine ions.

The F atoms are bonded only to the octahedral cation whereas the O atoms are bonded to both octahedral and tetrahedral cations. This fact explains why the F–F distance is shorter than the O–O distance. This was already remarked in our previous paper, for the OH groups. In the present fluormica we observe F–F = 2·629 ± 0·008 Å and O–O = 2·804 ± 0·008 Å in the octahedron around (Mg,Li)(2). The difference, 0·175 Å, between these two opposite shared edges is greater than the shortening, 0·038 Å, found from (Mg,Li)–O = 2·077 to (Mg,Li)–F = 2·039 Å. This fact

may account for the slight observed displacement of (Mg,Li)(2) away from the F–F shared edge, from $Y/b = 0{\cdot}3333$ to $Y/b = 0{\cdot}3308$, with standard deviation 0·0002.

Potassium deficiency

There is no reason to doubt that the vacant potassium sites are distributed at random. It is interesting to speculate on how they can affect the deformation of the tetrahedral sheets. Basal oxygen atoms are free to move in a direction parallel to the line that joins the nearest two potassium atoms (see Fig. 1 of Donnay, Donnay & Takeda, 1964). The vibration ellipsoid of a basal oxygen atom (for apparent anisotropic temperature factor) would be expected to be elongated in this direction.

The r.m.s. components of the apparent thermal displacements of atoms along the principal axes of the ellipsoid (computed by ORFFE program) show that, within three standard deviations, the temperature factors can be considered isotropic. For each of the basal oxygen atoms O(1) and O(2), we have calculated the lengths and directions of four vectors: the three principal semi-axes, $\mathbf{r}_1$, $\mathbf{r}_2$, $\mathbf{r}_3$, of the ellipsoid and the length of a component $\mathbf{r}_K$ parallel to the line that connects the nearest two potassium atoms. The direction of each $\mathbf{r}_i$ vector is given by the three angles, λ, μ, γ, that it makes with the axes of an auxiliary system of coordinates: γ, with c^*; λ, with the nearest K–K direction; μ, with a line perpendicular (or nearly perpendicular) to the first two. Note that for atom O(1), the auxiliary coordinate axes are directed along a, b, c^*; for atom O(2), they are along $\mathbf{a}-\mathbf{b}$, $3\mathbf{a}+\mathbf{b}$, $\mathbf{c}^*$, where vector $(3\mathbf{a}+\mathbf{b})$ is perpendicular to the plane $(\mathbf{a}-\mathbf{b}, \mathbf{c}^*)$ within a few minutes of arc. The results (Table 8 and Fig. 1) show that the ellipsoids are elongated nearly as expected.

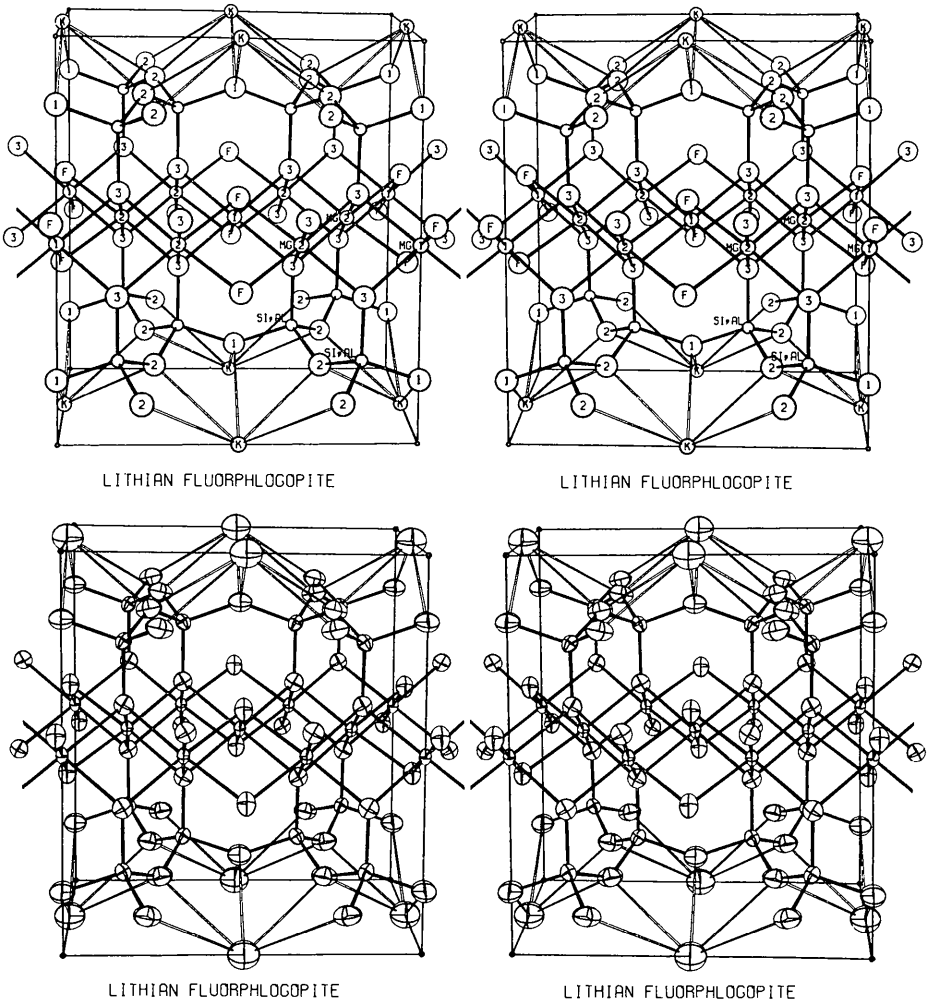

Fig. 1 (by Carroll K. Johnson). Stereoscopic drawings of the crystal structure showing the atomic centers (upper pair) and their thermal ellipsoids (lower pair). The atoms are numbered as on Table 3. The ellipsoids enclose 85 % of the probability distribution, as their axes are equal to 2·3 times the r.m.s. displacements.

The crystal setting is conventional: origin at the lower-left-back corner of the cell, $+\mathbf{c}$ vertical, $+\mathbf{a}$ sloping toward the observer, $+\mathbf{b}$ horizontal and to the right. The line of sight lies in a vertical plane and is inclined downwards at an angle of 5° to $-\mathbf{a}^*$.

Finally the determined structure was compared with the predicted structure. In our previous paper we prepared nomograms that predict the atomic coordinates in terms of chemical composition (whence d_t and d_o) and observed b. Our program, however, was written in such a way that the atomic coordinates were functions of b and $c \sin\beta = d(001)$. Even though agreement was found between observed and predicted values of bond lengths, s/u ratio, α, and ψ (Table 9), the disagreement on atomic coordinates may exceed 20 standard deviations. Many crystal-chemical features of the determined structure are not evident from the predicted one. Detailed determinations of additional key structures in the mica group are still desirable.

We wish to thank Dr E.W.Radoslovich (Division of Soils, C.S.I.R.O., Adelaide) for suggesting the problem; Dr J.L.Miller (U.S. Bureau of Mines, Norris, Tennessee) for the chemical analysis; Professor W.E. Love (Biophysics Department) for the use of the integrating Weissenberg camera. We are also indebted to Dr Charles W.Burnham (Geophysical Laboratory, Carnegie Institution of Washington) for use of the diffractometer, guidance in data collecting, help on the structure refinement, and critical reading of our manuscript; Dr H.M.Crosswhite (Physics Department) for use of the microphotodensitometer; Professor J.M. Stewart (University of Maryland) for help in computations; Dr Gabrielle Donnay (Geophysical Laboratory) for crystal-chemical discussions; to Dr Carroll K.Johnson for the preparation of the stereoscopic drawings. The refinement calculations were performed on IBM 7094 at the Computation Center of The Johns Hopkins University.

References

BURNHAM, C. W. (1963*a*). *Z. Kristallogr.* **118**, 127.
BURNHAM, C. W. (1963*b*). *An* IBM 709/7090 *computer program for computing transmission factors for crystals of arbitrary shape.* Geophysical Laboratory, Washington, D.C.
BURNHAM, C. W. (1965). *Amer. Min.* **50**, 282.
BUSING, W. R., MARTIN, K. O. & LEVY, H. A. (1962). *A Fortran crystallographic least-squares program,* ORNL-TM-305. Oak Ridge National Laboratory, Oak Ridge, Tennessee.
BUSING, W. R., MARTIN, K. O. & LEVY, H. A. (1964). *ORFFE,* ORNL-TM-3060. Oak Ridge National Laboratory.
DONNAY, G., MORIMOTO, N., TAKEDA, H. & DONNAY, J. D. H. (1964*a*). *Acta Cryst.* **17**, 1369.
DONNAY, G., DONNAY, J. D. H. & TAKEDA, H. (1964*b*). *Acta Cryst.* **17**, 1374.
DONNAY, J. D. H. & TAKEDA, H. (1964). *Science,* **143**, 1162.
FRANZINI, M. & SCHIAFFINO, L. (1963). *Z. Kristallogr.* **119**, 297.
International Tables for X-ray Crystallography (1962). Vol. III. Birmingham: Kynoch Press.
JOHNSON, C. K. (1965). ORTEP: *A Fortran thermal ellipsoid plot program for crystal structure illustrations.* Oak Ridge National Laboratory Report ORNL-3794.
KOHN, J. A. & HATCH, R. A. (1955). *Amer. Min.* **40**, 10.
MILLER, J. L. & JOHNSON, R. C. (1962). *Amer. Min.* **47**, 1049.
NORDMAN, C. E. & PATTERSON, A. L. (1957). *Rev. Sci. Instrum.* **28**, 384.
SMITH, J. V. & BAILEY, S. W. (1963). *Acta Cryst.* **16**, 801.
YAMZIN, I. I., TIMOFEYEVA, V. A., SHASHKINA, I. I., BELOVA, E. N. & GLIKI, N. V. (1955). *Mém. Soc. russe. Min.* (2) **84**, 415 (*Min. Abs.* **13**, 419).
YODER, H. S. & EUGSTER, H. P. (1954). *Geochim. et Cosmochim. Acta,* **6**, 157.

Acta Cryst. (1966). **20**, 646

Structure de l'Hydroxy-4-Coumarine. Eau d'Hydratation et Cohésion Cristalline

PAR JACQUES GAULTIER ET CHRISTIAN HAUW

Laboratoire de Cristallographie, Faculté des Sciences de Bordeaux, France

(*Reçu le* 16 *juillet* 1965)

The structure of 4-hydroxycoumarin monohydrate has been determined by a three-dimensional X-ray analysis with photographic data and refined by the least-squares method on an IBM 1620 computer; there are four molecules in the orthorhombic unit cell. Although the hydrogen atom positions have not been determined, it is believed that there are three hydrogen bonds between water molecules and 4-hydroxycoumarin molecules: O(H) $\cdots$ W = 2·59 Å, O $\cdots$ (H)W = 2·73 and 2·80 Å.

Nous décrivons ici la structure et l'organisation cristalline de l'hydroxy-4-coumarine que nous comparons à son homologue bromé-3 (Gaultier & Hauw, 1965*c*). Il était intéressant d'observer quel pouvait être l'aspect pris par l'hétérocycle en l'absence de brome. Le même intérêt pouvait se manifester au sujet de l'eau d'hydration qui était, dans le dérivé bromé, le facteur essentiel assurant la cohésion du cristal.